



Oct 23rd, 12:00 AM

A Simple Semi-analytical, Semi-numerical Approach to Thin-walled Structures Stability Problems

J. Rhodes

P. W. Khong

Follow this and additional works at: <https://scholarsmine.mst.edu/isccss>



Part of the [Structural Engineering Commons](#)

Recommended Citation

Rhodes, J. and Khong, P. W., "A Simple Semi-analytical, Semi-numerical Approach to Thin-walled Structures Stability Problems" (1990). *International Specialty Conference on Cold-Formed Steel Structures*. 4.

<https://scholarsmine.mst.edu/isccss/10iccfss/10iccfss-session2/4>

This Article - Conference proceedings is brought to you for free and open access by Scholars' Mine. It has been accepted for inclusion in International Specialty Conference on Cold-Formed Steel Structures by an authorized administrator of Scholars' Mine. This work is protected by U. S. Copyright Law. Unauthorized use including reproduction for redistribution requires the permission of the copyright holder. For more information, please contact scholarsmine@mst.edu.

A SIMPLE SEMI-ANALYTICAL, SEMI-NUMERICAL APPROACH TO THIN-WALLED STRUCTURES STABILITY PROBLEMS

James Rhodes¹ and P W Khong²

Abstract

A simple and efficient methodology has been developed to predict the elastic buckling behaviour of thin-walled structures. In the analysis, the cross section is treated as a system of connected plate and the buckling behaviour of each individual plate component is described. Utilizing the variational method based upon the principle of minimum potential energy, the stiffness of each plate component is then assembled based upon the methodology of matrix structural analysis. Unlike the Finite Element Method (FEM) and the Finite Strip Method (FSM), the proposed model is independent upon the mesh subdivision and intelligent use of experience. Although only one term solution for the trigonometric function is used as the deflection form in the longitudinal direction, it provides upper bound solutions that were found to be in reasonably good agreement with the existing published solutions.

Notation

b	Width of elemental strip
k	Buckling coefficient of structure
k_1	Buckling coefficient of the 1 st plate component
l	Length of structure
m	Number of half-waves in longitudinal direction
t	Strip, plate thickness
u, v, w	Displacements in x , y and z direction
$\omega(x, y)$	out-of-plane displacement at co-ordinate (x, y)
x, y, z	Cartesian coordinate
A_i	Cross-sectional area of strip
A	Cross-sectional area of structure
D	Flexural rigidity, ($D = E t^3 / (12(1 - \nu^2))$)
E	Young's Modulus or modulus of elasticity
N	Total number of strips/plate components of the structure
U_B	Strain energy due to bending
U_{BI}	In-plane strain energy in bending
U_{BO}	Out-of-plane strain energy in bending
V	Change in potential energy of a system
W_B	Work done due to external loading

1 Reader, Department of Mechanical and Process Engineering, University of Strathclyde, Montrose Street, Glasgow G1 1XJ, U.K.

Currently visiting professor of School of Mechanical and Production Engineering, Nanyang Technological Institute, Nanyang Avenue, SINGAPORE

2 Lecturer, School of Mechanical and Production Engineering, Nanyang Technological Institute, Nanyang Avenue, SINGAPORE

W_{BI}	Work done by in-plane bending
W_{BO}	Work done by out-of-plane bending
ν	Poisson's ratio of isotropic material, taken as 0.3 unless otherwise stated
θ_1, θ_2	Angular displacements in y direction
$\sigma_x, \sigma_y, \sigma_z$	Direct stress in the x, y and z direction
σ_{cr}	Critical compressive stress
λ	Eigenvalue
α	Compression eccentricity factor
$\{\delta\}$	displacement parameters vector
$[K]$	assembled stiffness matrix
$[S]$	assembled stability matrix
Primes denote differentiation with respect to x	

$$\frac{\partial^2 v(x, y)}{\partial x^2} = v''$$

Symbols that not listed here are defined throughout the text or figure where they first appear.

Introduction

Advancements in computer technology in recent years have promoted the evolution of structural analysis through numerical methods. However, in some cases, semi-numerical, semi-analytical approaches have been used as a substitute for the numerical method with the objective of saving in computing cost and input data preparation.

For prismatic structural members, the **FSM** as suggested by Cheung [1,2] results in significantly reduced matrix size compared to the ordinary **FEM**. In his analysis, a Fourier series/polynomial series solution algorithm was presented. Unlike the finite element method, the finite strip method only discretises the structure in the transverse direction. Thus, the effort of discretising the model is relatively much less in **FSM** to achieve comparable accuracy to the **FEM**.

Although the **FSM** algorithm of plate bending problem has been the subject of substantial research interest as demonstrated by a number of papers that have appeared in the literature over the past two decades, most of the **FSM** workers use the cubic finite strip for their analysis since the algebraic complexity of the method increases drastically as higher order terms are introduced. On the other hand, the applications of the conventional higher order analysis are often restricted to structures with constant thickness or material properties.

In the present analysis, the cross section of structure is treated as a system of connected plate components. Each plate component is modelled by a single elemental strip for which its characters and behaviour are described by a fifth degree polynomial shape function in the transverse direction and trigonometric (one term) displacement function in the longitudinal direction. The use of the high accuracy higher order shape functions in the transverse direction, permits accurate results using only a single strip for each plate component of the structure. Thus, the proposed model dramatically increases the accuracy of the analysis and minimises the input data preparation during modelling.

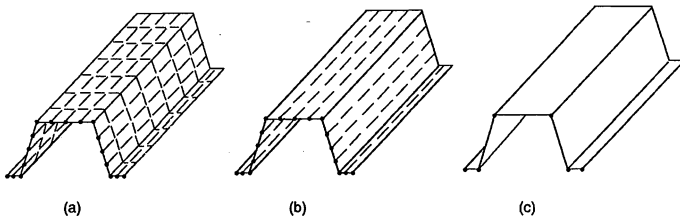


Fig.1 (a) Finite Element Model (b) Finite Strip Model (c) Proposed Model

Strain Energy

When subject to arbitrary external loads, the behaviour of each plate component can be analysed in terms of in-plane bending and out-of-plane bending effects. The knowledge of plate behaviour is thus essential. Utilizing the Love-Kichhoff assumption, the strain energy of a thin plate due to out-of-plane bending can be expressed as

$$U = \frac{D}{2} \int_A \left\{ \left[\frac{\partial^2 w}{\partial x^2} + \frac{\partial^2 w}{\partial y^2} \right]^2 + 2(1 - \nu) \left[\left(\frac{\partial^2 w}{\partial x \partial y} \right)^2 - \frac{\partial^2 w}{\partial x^2} \frac{\partial^2 w}{\partial y^2} \right] \right\} dA \quad (1)$$

Employing the energy approach based upon the Rayleigh-Ritz method, an assumed displacement function is chosen to satisfy the kinematic boundary conditions which involve rotations and translations in the transverse direction. In the present analysis, the displacement field is approximated by a fifth degree polynomial function which contains

a finite number of independent coefficients. In the longitudinal direction, a single term trigonometric function is assumed since the boundary conditions are known or pre-determined.

$$\begin{aligned}\omega(x, y) = & [w(1 - 10\eta^3 + 15\eta^4 - 6\eta^5) + b\theta_1(\eta - 6\eta^3 + 8\eta^4 - 3\eta^5) \\ & + 0.5b^2\kappa_1(\eta^2 - 3\eta^3 + 3\eta^4 - \eta^5) + W(10\eta^3 - 15\eta^4 + 6\eta^5) \\ & + b\theta_2(-4\eta^3 + 7\eta^4 - 3\eta^5) + 0.5b^2\kappa_2(\eta^3 - 2\eta^4 + \eta^5)] X\end{aligned}\quad (2)$$

In which $X = \sin(m\pi x/l)$

$$\eta = y/b$$

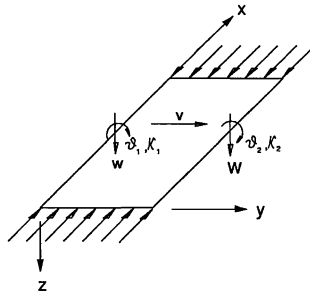


Fig.2 Displacement Configuration

Substituting the assumed displacement function into Eqn.(1) and differentiating with respect to the unknown displacement coefficients, the minimized strain energy of a plate component can be expressed as

$$\frac{\partial U_{BO}}{\partial(\{\delta\})} = \frac{Db}{14} \begin{bmatrix} P_{11} & & & & & \\ P_{21} & P_{22} & & & & \\ P_{31} & P_{32} & P_{33} & & & \\ P_{41} & P_{42} & P_{43} & P_{44} & & \\ P_{51} & P_{52} & P_{53} & P_{54} & P_{55} & \\ P_{61} & P_{62} & P_{63} & P_{64} & P_{65} & P_{66} \end{bmatrix} \begin{Bmatrix} w \\ b\theta_1 \\ W \\ b\theta_2 \\ b^2\kappa_1 \\ b^2\kappa_2 \end{Bmatrix} \quad (3)$$

where

$$P_{11} = \frac{181}{33}I_1 + 240I_2 + 40I_3$$

$$P_{21} = \frac{311}{330}I_1 + 120I_2 + 6I_3 - 14I_4$$

$$P_{31} = \frac{50}{33}I_1 - 240I_2 - 40I_3$$

$$P_{41} = -\frac{151}{330}I_1 + 120I_2 + 6I_3$$

$$P_{51} = \frac{281}{3960}I_1 + 6I_2 + \frac{1}{3}I_3$$

$$P_{61} = \frac{181}{3960}I_1 - 6I_2 - \frac{1}{3}I_3$$

$$P_{22} = \frac{104}{495}I_1 + \frac{384}{5}I_2 + \frac{32}{5}I_3$$

$$P_{32} = -P_{41}$$

$$P_{42} = -\frac{133}{990}I_1 + \frac{216}{5}I_2 + \frac{2}{5}I_3$$

$$P_{52} = \frac{23}{1320}I_1 + \frac{22}{5}I_2 + \frac{7}{15}I_3$$

$$P_{62} = \frac{13}{990}I_1 - \frac{8}{5}I_2 + \frac{2}{15}I_3$$

$$I_1 = \int_0^l (X'')^2 dx$$

$$I_2 = \int_0^l (X')^2 dx$$

$$I_3 = \int_0^l [(X')^2 - v(X')^2 - v(X \cdot X'')] dx$$

$$I_4 = \int_0^l X \cdot X'' dx$$

$$P_{33} = \frac{181}{33}I_1 + 240I_2 + 40I_3$$

$$P_{43} = -P_{21}$$

$$P_{53} = P_{61}$$

$$P_{63} = P_{51}$$

$$P_{44} = P_{22}$$

$$P_{54} = -P_{62}$$

$$P_{64} = -P_{52}$$

$$P_{55} = \frac{1}{660}I_1 + \frac{6}{5}I_2 + \frac{2}{45}I_3$$

$$P_{65} = \frac{1}{792}I_1 + \frac{1}{5}I_2 + \frac{1}{45}I_3$$

$$P_{66} = P_{55}$$

Matrix $[P]$ is symmetric and represents the stiffness of a plate component due to out-of-plane bending.

The in-plane destabilizing effects of the basic stress system is derived as in [3,4] using elementary beam theory. For thin-walled open section under some arbitrary external loading system as shown in Fig.3, the assumption made is that the membrane stress system vary linearly across each strip component due to bending.

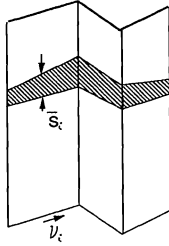


Fig.3 Stress System Due To In-Plane Bending

Treating each plate component as a single beam element, the longitudinal stress of i th plate can be expressed as

$$\begin{aligned} S_i &= \bar{S}_i + E y_i \frac{\partial^2 v(x, y)}{\partial x^2} \\ &= \bar{S}_i + E v''_i y_i \end{aligned} \quad (4)$$

In which $v(x, y) = v \cdot X$ is the in-plane displacement, v'' is the in-plane curvature and \bar{S}_i is the average longitudinal stress.

Since the transverse and shear stress can be disregarded in the beam theory and the in-plane displacements considered are due solely to in-plane bending, the resultant end load on any section must be zero.

$$\sum_{i=1}^N S_i A_i = 0 \quad (5)$$

And the in-plane bending strain energy of a system of plate components is given by

$$U_{BI} = \sum_{n=1}^N \frac{1}{2} \int_V \frac{S_n^2}{E} dV \quad (6)$$

Employing the Rayleigh-Ritz method and minimising the last expression with respect to the displacement coefficients, the minimized strain energy of structure due to in-plane bending is

$$\begin{aligned}
\frac{dU_{BI}}{dv_i} &= \sum_{n=1}^N \frac{dU_n}{dv_i} \\
&= \frac{EI_1 b_i}{4} \left\{ \sum_{\substack{j=1 \\ j \neq i}}^N \left[\bar{A} - \frac{(\bar{A}_i - \underline{A}_i)(\bar{A}_j - \underline{A}_j)}{A} \right] v_j b_j + \left[A - \frac{2}{3} b_i t_i - \frac{(\bar{A}_i - \underline{A}_i)^2}{A} \right] v_i b_i \right\} \\
&= [E] \{\delta_i\}
\end{aligned} \tag{7}$$

where

$$\begin{aligned}
A_k &= b_k t_k, \quad \bar{A}_i = \sum_{k=i+1}^N b_k t_k, \quad \underline{A}_i = \sum_{k=1}^{i-1} b_k t_k \\
\bar{A} &= \sum_{k=1}^{j-1} A_k + \sum_{k=i+1}^N A_k - \sum_{k=j+1}^{i+1} A_k
\end{aligned}$$

Potential Loss

In deriving the stability matrix of external forces, it is assumed that each load is applied gradually until its critical value is reached and that each load-displacement relationship is linear. Considering a plate component of width dy loaded by $\sigma_x t dy$ as shown,

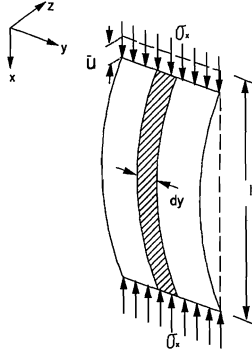


Fig. 4 Plate Subjected To Uniform End Compression

The effective shortening in the x -direction can be approximated by

$$\bar{u} = \int_0^l \frac{d\bar{u}}{dx} dx \approx \frac{1}{2} \int_0^l \left(\frac{\partial w}{\partial x} \right)^2 dx \tag{8}$$

For a series of connected plates, each with different compressive eccentricity factor α , the applied stress of i th plate is given by

$$\sigma_i = \sigma_0 \left(\beta_i - \alpha_i \frac{y_i}{b_i} \right)$$

where $\beta_i = 1 - \sum_{j=1}^{i-1} \alpha_j$

In which σ_0 is the stress at the origin of 1st plate. The work done by system of external loads that produce the deformation is finally expressed as

$$W = \frac{\sigma_0 t}{2} \int_{A_i} \left(\beta_i - \frac{\alpha_i y_i}{b_i} \right) \left(\frac{\partial w}{\partial x} \right)^2 dA \quad (9)$$

Substituting Eqn.(2) into Eqn.(9) and differentiating with respect to the displacements coefficients, the minimized potential loss due to out-of-plane bending is

$$\frac{\partial W_{BO}}{\partial(\{\delta\})} = \frac{\sigma_0 t b}{42} \begin{bmatrix} Q_{11} & & & & & \\ Q_{21} & Q_{22} & & & & \\ Q_{31} & Q_{32} & Q_{33} & & & \\ Q_{41} & Q_{42} & Q_{43} & Q_{44} & & \\ Q_{51} & Q_{52} & Q_{53} & Q_{54} & Q_{55} & \\ Q_{61} & Q_{62} & Q_{63} & Q_{64} & Q_{65} & Q_{66} \end{bmatrix} \begin{Bmatrix} w \\ b\theta_1 \\ W \\ b\theta_2 \\ b^2\kappa_1 \\ b^2\kappa_2 \end{Bmatrix} I_s \quad (10)$$

where

$$\begin{aligned} Q_{11} &= \frac{181}{11}\beta - \frac{41}{11}\alpha & Q_{33} &= \frac{181}{11}\beta - \frac{420}{33}\alpha \\ Q_{21} &= \frac{311}{110}\beta - \frac{289}{330}\alpha & Q_{43} &= -\frac{311}{110}\beta + \frac{966}{495}\alpha \\ Q_{31} &= \frac{50}{11}\beta - \frac{25}{11}\alpha & Q_{53} &= \frac{181}{1320}\beta - \frac{21}{280}\alpha \\ Q_{41} &= -\frac{151}{110}\beta + \frac{107}{165}\alpha & Q_{63} &= \frac{281}{1320}\beta - \frac{273}{1980}\alpha \\ Q_{51} &= \frac{281}{1320}\beta - \frac{21}{280}\alpha & Q_{44} &= \frac{104}{165}\beta - \frac{399}{990}\alpha \\ Q_{61} &= \frac{181}{1320}\beta - \frac{41}{660}\alpha & Q_{54} &= -\frac{13}{330}\beta + \frac{63}{3080}\alpha \\ Q_{22} &= \frac{104}{165}\beta - \frac{5}{22}\alpha & Q_{64} &= -\frac{23}{440}\beta + \frac{21}{660}\alpha \\ Q_{32} &= \frac{151}{110}\beta - \frac{239}{330}\alpha & Q_{55} &= \frac{1}{220}\beta - \frac{1}{528}\alpha \\ Q_{42} &= -\frac{399}{990}\beta + \frac{399}{1980}\alpha & Q_{65} &= \frac{1}{264}\beta - \frac{1}{528}\alpha \end{aligned}$$

$$Q_{52} = \frac{23}{440}\beta - \frac{63}{3080}\alpha$$

$$Q_{53} = \frac{13}{330}\beta - \frac{5}{264}\alpha$$

$$Q_{55} = \frac{1}{220}\beta - \frac{21}{7920}\alpha$$

$$I_5 = \int_0^l (X')^2 dx$$

The derivation of potential loss due to in-plane bending is similar to the out-of-plane bending but the in-plane deformations are considered.

$$\begin{aligned} \frac{\partial W_{BI}}{\partial v_i} &= \sigma_o t b \left(\beta - \frac{\alpha}{2} \right) I_5 v_i \\ &= [H] \{ \delta_i \} \end{aligned} \quad (11)$$

Transformation of Displacement Fields

In the formation of the overall structural stiffness matrix, it is advantageous to write the element stiffness matrices in terms of the in-plane displacements rather than the out-of-plane displacements.

Considering an open section under some arbitrary external loading system, the connected edge, node P is assumed moving to a new coordinate P' as shown in the following figure,

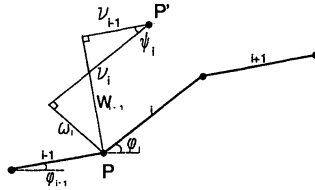


Fig.5 Displacement Configuration

In which $\psi_i = \phi_i - \phi_{i-1}$. The new position represents the effect of the combination of both out-of-plane and in-plane bending imposed on the system. The assumption made here is that there is no axial strain in the local y -direction of each plate component.

In Fig.5, from the geometry and trigonometry rules, the following relations of out-of-plane and in-plane displacement parameters arise.

$$w_i = v_i \cot \psi_i - v_{i-1} \operatorname{cosec} \psi_i$$

$$W_i = v_{i+1} \operatorname{cosec} \psi_{i+1} - v_i \cot \psi_{i+1} \quad (12)$$

which enable the out-of-plane displacement vector $\{w, b\theta_1, W, b\theta_2, b^2\kappa_1, b^2\kappa_2\}^T$ and in-plane displacement vector $\{v\}$ to be transformed to the new displacement vector $\{v_{i-1}, b\theta_1, v_i, b\theta_2, v_{i+1}, b^2\kappa_1, b^2\kappa_2\}^T$

Total Potential Energy

Employing the Rayleigh-Ritz method, the potential energy is a minimum at equilibrium. This leads to the derivatives of the energy with respect to the new displacement parameters $\{v_{i-1}, v_i, v_{i+1}, b\theta_1, b\theta_2\}^T$, which are

$$\frac{\partial U}{\partial(v_{i-1})} = \frac{\partial U}{\partial(w)} \frac{\partial(w)}{\partial(v_{i-1})} + \frac{\partial U}{\partial(W)} \frac{\partial(W)}{\partial(v_{i-1})}$$

$$\frac{\partial U}{\partial(v_i)} = \frac{\partial U}{\partial(w)} \frac{\partial(w)}{\partial(v_i)} + \frac{\partial U}{\partial(W)} \frac{\partial(W)}{\partial(v_i)}$$

$$\frac{\partial U}{\partial(v_{i+1})} = \frac{\partial U}{\partial(w)} \frac{\partial(w)}{\partial(v_{i+1})} + \frac{\partial U}{\partial(W)} \frac{\partial(W)}{\partial(v_{i+1})} \quad (13)$$

Substituting Eqn.(3) and the derivatives of Eqn.(12) into Eqn.(13), the modified derivatives of the strain energy with respect to the new displacements fields are given by

$$\frac{\partial U_b}{\partial(\{\delta\}_e)} =$$

$P_{11}C_i^2$	$-P_{12}C_i$	$-P_{11}C_iT_i + P_{13}C_iT_{i+1}$	$-P_{14}C_i$	$-P_{13}C_iC_{i+1}$	$-P_{15}C_i$	$-P_{16}C_i$
	P_{22}	$P_{21}T_i - P_{23}T_{i+1}$	P_{24}	$P_{23}C_{i+1}$	P_{25}	P_{26}
		$E_i + P_{13}T_i^2 + P_{33}T_{i+1}^2 - 2P_{13}T_iT_{i+1}$	$P_{14}T_i - P_{34}T_{i+1}$	$-P_{33}T_{i+1}C_{i+1} + P_{13}T_iC_{i+1}$	$P_{15}T_i - P_{35}T_{i+1}$	$P_{16}T_i - P_{36}T_{i+1}$
			P_{44}	$P_{43}C_{i+1}$	P_{45}	P_{46}
				$P_{33}C_{i+1}^2$	$P_{35}C_{i+1}$	$P_{36}C_{i+1}$
					P_{55}	P_{56}
						P_{66}

sym.

$\{\delta\}_e$

$$= [K] \{\delta\}_e \quad (14)$$

where $c_i = \text{cosec } \psi_i$

$T_i = \cot \psi_i$

$\{\delta\}_e = \{v_{i-1}, b\theta_1, v_i, b\theta_2, v_{i+1}, b^2\kappa_1, b^2\kappa_2\}^T$

E_i is the element of $[E]$ in Eqn.(7)

Similarly, the displacement vector of potential energy loss due to out-of-plane bending in Eqn.(10) can be treated in the same way. After adding the potential energy loss due to in-plane bending from Eqn.(11), the potential energy loss due to edge loading of a plate component is given by

$$\frac{\partial W_B}{\partial \{\delta\}_e} = \begin{bmatrix} Q_{11}c_i^2 & -Q_{12}c_i & -Q_{11}c_iT_i + Q_{13}c_iT_{i+1} & -Q_{14}c_i & -Q_{13}c_ic_{i+1} & -Q_{15}c_i & -Q_{16}c_i \\ & Q_{22} & Q_{21}T_i - Q_{23}T_{i+1} & Q_{24} & Q_{23}c_{i+1} & Q_{25} & Q_{26} \\ & & H_i + Q_{11}T_i^2 + Q_{33}T_{i+1}^2 - 2Q_{13}T_iT_{i+1} & Q_{14}T_i - Q_{34}T_{i+1} & -Q_{33}T_{i+1}c_{i+1} + Q_{13}T_ic_{i+1} & Q_{15}T_i - Q_{35}T_{i+1} & Q_{16}T_i - Q_{36}T_{i+1} \\ & & & Q_{44} & Q_{43}c_{i+1} & Q_{45} & Q_{46} \\ & & \text{sym.} & & Q_{33}c_{i+1}^2 & Q_{35}c_{i+1} & Q_{36}c_{i+1} \\ & & & & & Q_{55} & Q_{56} \\ & & & & & & Q_{66} \end{bmatrix} \{\delta\}_e \quad (15)$$

In which H_i is the element of $[H]$ matrix derived from Eqn.(11) that is due to the effect of in-plane bending stresses. These can be directly added on the v_i displacement parameters of the stability matrix.

Eqns.(14) and (15) establish the stiffness matrix and stability matrix respectively for each plate component. By analogy, with the element stiffness and stability matrices, the

relationship between external loads on the structure and displacement of joints of the structure is known as structural stiffness matrix. For buckling, the characteristic eigenvalue problem is formed as follows.

$$[K] \{\delta\} - \lambda[S] \{\delta\} = 0 \quad (16)$$

Where $[K]$ is the assembled stiffness matrix, $[S]$ is the assembled stability matrix and λ is the characteristic eigenvalue or critical load factor. Generally, the transcendental equation has an infinite number of roots. To represent the stability criterion, the smallest root is the critical load factor at which the structure passes from its stable position to a deformed configuration.

The assembly algorithm is of fundamental importance in the present analysis and is shown graphically in Fig.6.

$$\begin{bmatrix} 1 & 1 & 1 & 1 & 1 & & & 1 & 1 & & \\ 1 & 1 & 1 & 1 & 1 & & & 1 & 1 & & \\ 1 & 1 & 2 & 2 & 2 & 2 & 2 & 1 & 1 & 2 & 2 \\ 1 & 1 & 2 & 2 & 2 & 2 & 2 & 1 & 1 & 2 & 2 \\ 1 & 1 & 2 & 2 & 3 & 3 & 3 & 3 & 3 & 1 & 1 \\ & & 2 & 2 & 3 & 3 & 3 & 3 & 3 & 2 & 2 \\ & & 2 & 2 & 3 & 3 & 3 & 3 & 3 & 2 & 2 \\ & & & 3 & 3 & 3 & 3 & 3 & 3 & 3 & 3 \\ & & & 3 & 3 & 3 & 3 & 3 & 3 & 3 & 3 \\ & & & & 3 & 3 & 3 & 3 & 3 & 3 & 3 \\ 1 & 1 & 1 & 1 & 1 & & & 1 & 1 & & \\ 1 & 1 & 1 & 1 & 1 & & & 1 & 1 & & \\ & & 2 & 2 & 2 & 2 & 2 & & 2 & 2 & \\ & & 2 & 2 & 2 & 2 & 2 & & 2 & 2 & \\ & & & 3 & 3 & 3 & 3 & & 3 & 3 & \\ & & & 3 & 3 & 3 & 3 & & 3 & 3 & \end{bmatrix} \begin{pmatrix} U_0 \\ \psi_1 \\ U_1 \\ \psi_2 \\ U_2 \\ \psi_3 \\ U_3 \\ \psi_4 \\ U_4 \\ K_1 \\ K_2 \\ K_1 \\ K_2 \\ K_1 \\ K_2 \end{pmatrix}$$

Fig.6 Overall Matrix Assembling

The above figure shows the method of three plate components' stiffness matrices assembling to form a structural matrix. The size of matrix of this proposed model is $4N+3$ and is the mathematical expression of compatibilities at the joints of structure. The curvatures at the interface between neighbouring plate component are discontinuous. The discontinuous curvatures remove the constraints on the displacements and decrease the stiffness with respect to the finite number of coordinates used to describe the displaced configurations of the structure. Hence, energy increases when such constraints are removed and converges to a more accurate solutions.

In utilising edge curvatures as the element of the displacement vector, it may be thought that continuity at the boundaries with regard to curvature of adjacent plates must be satisfied for a mathematically admissible solution. However this is not the case as there is no requirement that curvature continuity be ensured. Indeed, curvature is related to the equilibrium conditions at the edges of plate component and equilibrium need not be enforced. If strict attention is paid to the equilibrium boundary conditions with regards to curvature, then significantly increased labour is required and the only result of this increased labour is that the solution produced is a higher upper bound (i.e. less accurate) than if the curvatures are allowed to vary so as to find the overall minimum of potential energy.

This is one of the relatively few occasions in which neglect of boundary conditions not only leads to a substantial reduction in labour, but also improves the accuracy of solution and also generalises the approach to deal with discontinuous thickness structures without any additional requirements.

Examples

Of greatest practical significance, the direct assembly of the matrix solution permits structures of non-constant thickness and material properties to be modelled. The accuracy and versatility of this algorithm are demonstrated in Table 1 and Fig.7 to Fig.10 in comparison to those of known analytical results.

Aspect Ratio	0.2	0.4	0.6	0.8	1.0	1.2	1.4
Bulson [5]	27.040	8.410	5.138	4.202	4.000	4.134	4.470
Present Analysis	27.040	8.410	5.138	4.203	4.001	4.135	4.471

Table 1 Buckling coefficient of axially loaded plate with all edges simply support

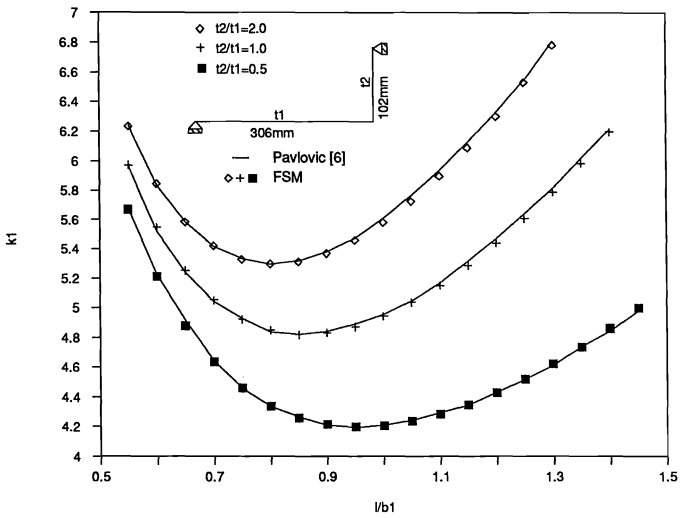


Fig.7 Buckling Of Uniformly Compressed Angle Column

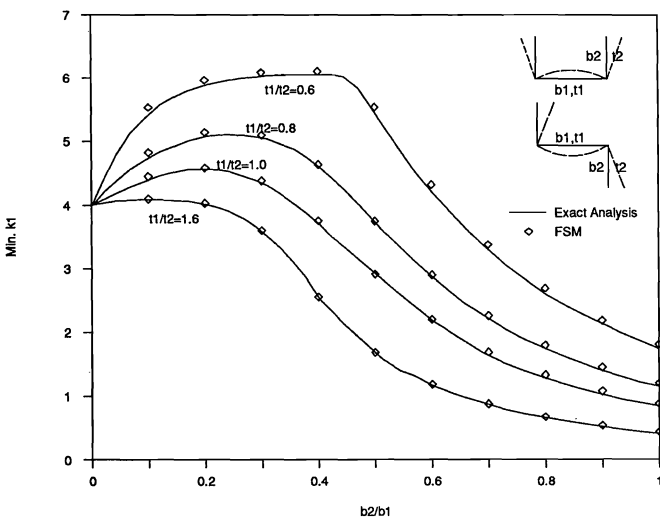


Fig.8 Elastic Buckling Solution Of Channel/Z-section

From these results, the predicted buckling solutions using the present analysis are in good agreement with the published solutions. Some discrepancies were apparent due to errors during the digitized tracing procedure.

Beside saving in machine computing time, the present methodology makes modelling versatile and thus any thin-walled structures can be modelled with much less effort compared to finite element method and lower order finite strip analysis. After extensive experience, the authors have found that the advantages of the proposed model outweighs the disadvantages.

The formulation using numerical/semi-numerical approach enables complex geometry and boundary conditions to be simulated by a mathematical model. In Fig.9, an asymmetry compound lip element is modelled with various boundary conditions along plate component. The elastic buckling solution for each of these conditions is represented in terms of the plate buckling coefficient.

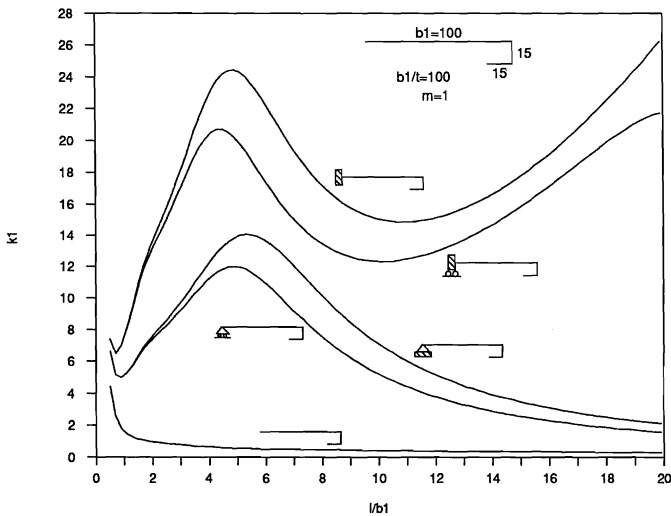


Fig.9 Buckling of Axially Compressed Compound Lip with Various Boundary Conditions Along Unloaded Plate Edge

Analytical approaches to the elastic buckling solutions of a stiffened channel section are tedious and are generally restricted to a specified geometric configuration. Using the present algorithm, the instability studies of the geometry of an intermediate stiffener of three channel sections are given in Fig.10. In the figure, the effects of three types of stiffener cross section are studied; rectangular, triangular and trapezoidal.

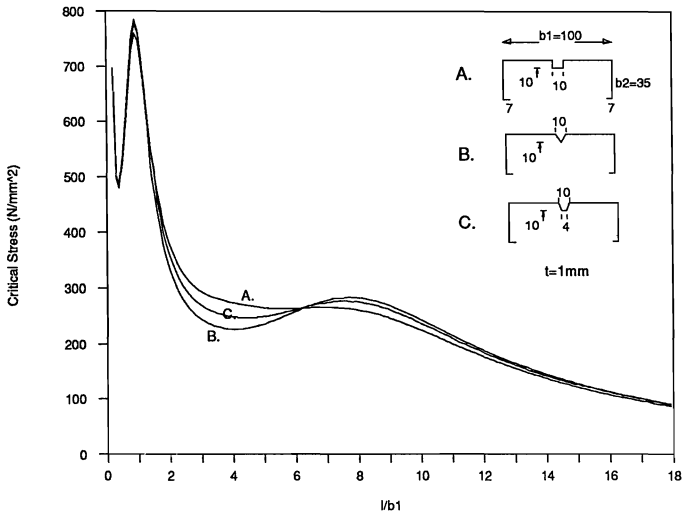


Fig.10 Buckling Stresses for Compressed Channels with Intermediate Stiffener

Conclusions

The proposed methodology is based upon an energy formulation which combines the modelling versatility of the contemporary finite strip approach in conjunction with the Rayleigh-Ritz method. However, it does not rely on small mesh subdivision and intelligent use of experience for accuracy. In general, it is found that the quintic shape function is capable of representing the true buckling deformations accurately across the structural cross section. Although a single term solution for the trigonometric function is used in the longitudinal direction, the approximation provides upper bound solutions that were found to be in good agreement with the existing published solutions.

References

- [1] Cheung Y.K., "The finite strip method in the analysis of elastic plates with two opposite simply supported ends", Proc.Inst.Civ.Eng., 40(1968), 1-7
- [2] Cheung Y.K., "Finite strip method in structural analysis", Pergammon Press, 1976
- [3] Rhodes J., "A simple microcomputer finite strip analysis", "Dynamics of structures", Proc. Of the session at structures congress'87 related to dynamics of structures, ASCE(1987), 276-291
- [4] Khong P.W. And Rhodes J., "Linear and non linear analysis on the micro using finite strips", "SAM'88 stress analysis and the micro", IOP publishing Ltd., 1988
- [5] Bulson P.S., "The stability of flat plates", Chatto & windus, London(1970)
- [6] Pavlovic M.N., "Buckling and vibration of plate assemblies of non-constant thickness", Thin-walled structures, 5(1987), 191-209

